

Development of FMCW Radar Signal Processing for High-Speed Railway Collision Avoidance

Farra Anindya Putri^a, Dayat Kurniawan^{b,*}, Rahmawati Hasanah^a,
Taufiqurrahman^{b,c}, Eko Joni Pristianto^b, Hana Arisesa^{b,c}, Yusuf Nur Wijayanto^d,
Deni Permana^b, Winy Desvasari^b, Ken Paramayudha^b, Arief Budi Santiko^b,
Dadin Mahmudin^{b,c}, Pamungkas Daud^b, Fajri Darwis^b, Erry Dwi Kurniawan^b,
Arie Setiawan^{b,e}, Tajul Miftahushudur^{b,f}, Prasetyo Putranto^{b,g}, Syamsu Ismail

^aDepartement of Electronic Engineering
Bandung State Polytechnic
Jl. Gegerkalong Hilir Ds. Ciwaruga
Bandung, Indonesia

^bResearch Center for Telecommunication
National Research and Innovation Agency
Komplek BRIN Jl. Sangkuriang No. 21
Bandung, Indonesia

^cFaculty of Electrical Engineering
Universiti Teknologi Malaysia
81310 Johor, Malaysia

^dResearch Center for Electronic
National Research and Innovation Agency
Komplek BRIN Jl. Sangkuriang No. 21
Bandung, Indonesia

^eGraduate School of Engineering
Mie University
1577 Kurimamachiya-cho Tsu city
Mie 514-8507, Japan

^fDepartment of Electrical and Electronic Engineering
The University of Manchester
Manchester, M13 9PL, UK
Manchester, United Kingdom

^gSchool of Electrical Engineering and Computer Science
KTH Royal Institute of Technology
SE-100 44 Stockholm, Sweden

Abstract

Collision is the main issue in safe transportation, including in the railway system. Sensor systems have been developed to detect obstacles to prevent a collision, such as using cameras. One disadvantage of the camera systems is that performance detection decreases in a not clean environment, like the target position behind the fogs. This paper discusses the development of frequency modulated continuous wave (FMCW) radar signal processing for high-speed railway collision avoidance. The development of radar signal processing combines a two-dimensional constant false alarm rate (2D-CFAR) and robust principal component analysis (RPCA) to detect moving targets under clutter. Cell average (CA) and Greatest of CA (GOCA) CFAR are evaluated under a cluttered wall environment along the railway track. From the experiment, the development of FMCW radar can detect stationary or moving obstacles around 675 meters in front of the locomotive. Combining 2D-CFAR and RPCA algorithm outperforms average background subtraction in extracting moving targets from strong clutter signals along the railway track.

Keywords: railway system, FMCW radar, collision avoidance, clutter removal, 2D-CFAR, RPCA.

I. INTRODUCTION

Developing sensor technology to minimize collision is mandatory in transportation systems, including the

railway system. Train collisions are caused by cracked tracks, a collision between trains and obstacles, or a collision between trains on the same track. Combining position sensors such as GPS and wireless communication has been developed to prevent a collision [1]-[4]. The train position is reported between trains, train and control centers through wireless communication networks such as GSM and Wi-Fi. The performance of this system depends on GPS accuracy and GSM or Wi-Fi networks along railway tracks. In another way,

* Corresponding Author.

Email: daya004@brin.go.id; daysdk63@gmail.com

Received: June 27, 2022 ; Revised: August 8, 2022

Accepted: August 12, 2022 ; Published: August 31, 2022

Open access under CC-BY-NC-SA

© 2022 BRIN

cameras and range sensors have been developed to detect railway track obstacles [5]-[8]. The image processing technique and machine learning identify obstacles along the railway track. The result shows that the system can detect obstacles in a clean environment within a specific range. While in [9], 3D-Lidar Internet of Thing (IoT) is used for surveillance systems in the railway crossing area. Vision sensor performance mentioned above depends on environmental conditions, such as decreasing performance detection when obstacles inside fog and is limited in detection range.

A radar system is one of the detection systems developed to overcome the problem mentioned above. Radar application in railway systems has advantages in long-range detection, insensitivity to weather conditions, and good accuracy and resolution [10]. Frequency modulated continuous wave (FMCW) is one type of radar with advantages in accuracy for short-range measurements, low sensitivity to noise/clutter interference, and low power consumption. Implementing a radar system for railway collision avoidance has been introduced in [11]. The system detection consists of radar and a camera to improve obstacle performance detection. Kalman filter tracks a target and achieves a detection range up to 600m.

In railway collision avoidance systems, in a case due to obstacles or trains on the same track, the minimum obstacle detection range is a primary concern behind the engine brake system. This minimum detection range guarantees that the engine braking system can handle the train to stop in safe conditions. The minimum range detection for high-speed trains with a 300 km/ hour velocity is 2700 m [12]-[13]. Radar system design to meet that requirement is still challenging in recent years. In [12], introduce radar system design with a multiple receiver antenna with a minimum detection range of 3000 meters to prevent a collision. That system achieves a detection range up to 1000m with cell averaging constant false alarm rate (CA-CFAR) as the detection algorithm. With multiple receiver antenna, it implies to complexity algorithm and needs more cost.

The minimum range detection is a mandatory requirement to prevent a collision. Conversely, the targets are usually mixed with a cluttered environment, such as clutter from building along the railway track. Clutter removal and moving target detection algorithms become primary issues in this field. CFAR algorithms commonly detect targets under noise and in cluttered environments. CA-CFAR is introduced to detect targets with low processing time and exemplary performance in a homogeneous environment [14] but poorly in a non-homogeneous environment [15]. The greatest of CA (GOCA) CFAR is proposed to tackle detection performance in a non-homogeneous environment [16]. Moving target detection under clutter and noise is still a challenge. A moving target indication (MTI) filter introduce to detect a slow-moving target [17]. Slow-moving target detection under a cluttered environment using robust principal component analysis (RPCA) is

presented in [18], [19]. RPCA outperforms MTI due to RPCA can suppress clutter effectively and possibly prevent moving targets. The essential operation of RPCA is to extract a data matrix into a low-rank clutter matrix and a sparse moving targets matrix.

This work is initial research to develop radar obstacle detection for a high-speed train in Indonesia. This paper focused on radar signal processing development to prevent a collision along the railway track. Two problems to be solved in this research are the minimum detection range of 3000 meters and clutter removal along the railway track. To achieve that, combining CFAR and RPCA is proposed. Two-dimensional CFAR (2D-CFAR) is used to detect targets under noise clutter, while RPCA algorithm removes strong clutter that cannot be removed by CFAR processing.

II. FMCW RADAR

A. FMCW Radar Architecture

In general, the development of FMCW radar for high-speed railway collision avoidance is shown in Figure 1. The FMCW radar consists of several main components such as a synchronized clock 50 Mhz, coupler, linear frequency modulated (LFM) chirp generator, power amplifier (PA), antennas, low noise amplifier (LNA), mixer, voltage gain amplifier (VGA), low pass filter (LPF), analog-to-digital converter (ADC) and personal computer (PC). LMF chirp generator produce saw tooth form with bandwidth of 54 MHz to achieve maximum detection range. LFM chirp generator based on phase lock loop (PLL) and voltage control oscillator (VCO) to create stability of chirp signal compared to uncontrolled VCO. PA is used to increase signal power in the radar transmitter by around 500 mW. The antenna receiver and transmitter are designed using a microstrip array with twenty patches for each antenna. The received signal from targets depends on the distance between targets and radar. Generally received signal is too low, and LNA is used to increase the received signal to a certain level. FMCW radar used beat frequency to determine the target range. The beat frequency is captured from the output I/Q mixer. The received signal in the I/Q form is digitalized using an analog-to-digital converter (ADC) board with 12 bits resolution. From the digitalized signal, pre-processing, range processing, target detector, and clutter removal are implemented to determine targets along a railway track.

B. Constant False Alarm Rate (CFAR)

The Constant False Alarm Rate (CFAR) is a basic detection algorithm applied to the received signal of the radar. This algorithm determines a fixed threshold based on the background noise. If any sample exceeds the estimated threshold level, it is declared as the target is present, and others are declared as the target is not present. The critical elements of a CFAR detector are illustrated in Figure 2.

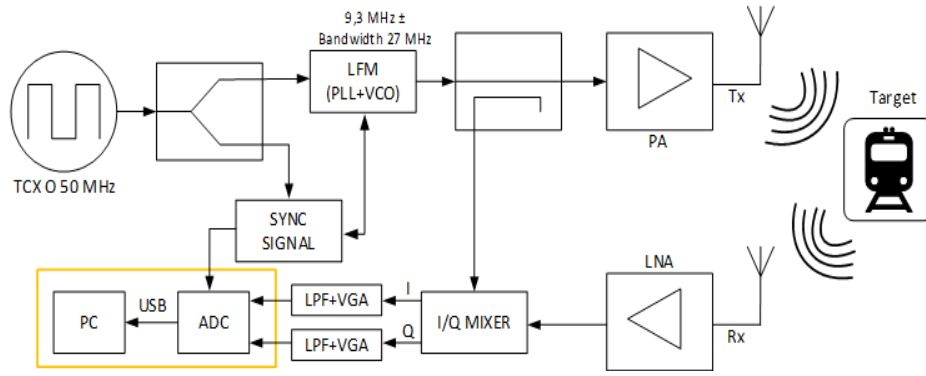


Figure 1. FMCW radar design system

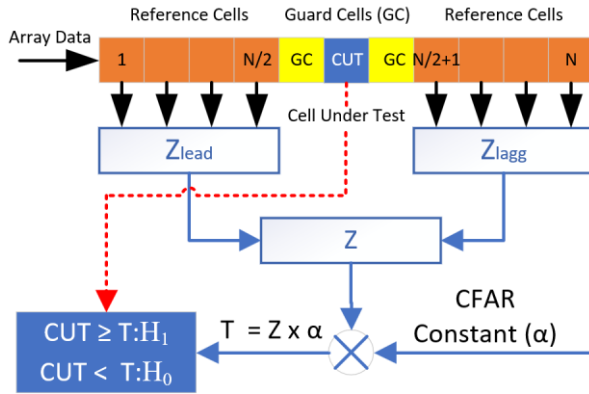


Figure 2. CFAR structure

- The Cell Under Test (CUT) is where the threshold is to be applied based on which the target is declared present or not.
- The guard cells (GC) are used to estimate the threshold in CUT precisely.
- The samples reference cells are used for the estimation of the noise level, thereby helping in calculating the threshold.

1) Cell Averaging CFAR (CA-CFAR)

CFAR algorithms have many types; one generally used is cell averaging CFAR (CA-CFAR) [14]. CA-CFAR has advantages in low complexity processing and better performance for single target detection in a homogenous environment. Calculating the CFAR constant or scale factor α_{CA} with the following formula as presented in (4)

$$Z_{lead} = \frac{2}{N} \sum_{i=1}^{N/2} X_i \quad (1)$$

$$Z_{lagg} = \frac{2}{N} \sum_{i=N/2+1}^N X_i \quad (2)$$

$$Z_{CA} = \frac{(Z_{lead} + Z_{lagg})}{2} \quad (3)$$

$$\alpha_{CA} = N \left(P_{fa}^{-\frac{1}{N}} \right) - 1 \quad (4)$$

where P_{fa} denoted probability false alarm rate, and N represent the total number of the reference cells. CA-CFAR threshold is calculated from averaging data of reference cell multiplied with scale factor. Form (4), the performance of CA-CFAR depends on determined P_{fa} value. In the detection system, the probability of detection (P_d) value is indicated of detection probability of the target is present and can be calculated from signal to noise ratio (SNR) value as (5) [20].

$$P_d = \left(1 + \frac{\alpha_{CA}}{N(1 + SNR)} \right)^{-N} \quad (5)$$

2) Greatest of CA-CFAR (GOCA-CFAR)

The greatest of CA-CFAR (GOCA-CFAR) was developed to improve the performance of CA-CFAR in a non-homogeneous environment [16]. The non-homogeneous environment is caused by clutter from the surrounding area, such as reflections from buildings. Unlike CA-CFAR, the GOCA-CFAR algorithm takes the maximum value of average power between the leading and lagging window, as presented in (6). The relation between P_{fa} and the scaling factor α_{GOCA} is defined as (7) [17].

$$Z_{GOCA} = \max(Z_{lead}, Z_{lagg}) \quad (6)$$

$$P_{fa} = \frac{1}{2} \left(1 + \frac{\alpha_{GOCA}}{N/2} \right)^{-N/2} \frac{1}{2} \left(1 + \frac{\alpha_{GOCA}}{N/2} \right)^{-N/2} \left\{ \sum_{k=0}^{N/2-1} \binom{N/2-1+k}{k} \left(2 + \frac{\alpha_{GOCA}}{N/2} \right)^{-k} \right\} \quad (7)$$

3) Two-dimensional CFAR

A two-dimensional CFAR (2D-CFAR) algorithm is presented in [21] to achieve low computational complexity but still outperforms the detection of one-dimensional (1D) CFAR in the radar data matrix (RDM). An RDM is composed of $Q \times R$ data matrix, where Q and

R denote target range and doppler, respectively. Assuming that the B-scan or range profile image is similar to RDM but the doppler matrix is substituted with frame numbers, 2D-CFAR can be implemented for the B-Scan matrix. Unlike with 1D-CFAR, the reference window in 2D-CFAR contains $K \times L$ cells around the cell under test. The reference window is shifted in range and frame numbers direction. The size of $K \times L$ cells is an essential parameter of detection performance because those cells are used to estimate the noise floor for the cell under test. 2D-CFAR structure based on a B-scan image is presented in Figure 3.

C. Robust Principal Component Analysis

The robust principal component analysis (RPCA) technique focuses on a matrix's decomposition into a low-rank and sparse matrix. In recent years, RPCA has been used in ground penetrating radar (GPR) and synthetic aperture radar (SAR) applications to remove background noise [18], [19], [22]. A B-Scan or range profile image is composed of several A-Scan into a two-dimensional matrix. Observed data matrix \mathbf{D} from B-scan image data can be presented as

$$\mathbf{D} = \mathbf{L} + \mathbf{S} + \mathbf{N} \quad (8)$$

where \mathbf{L} , \mathbf{S} , and \mathbf{N} denote a low-rank matrix of clutter, a sparse matrix of moving targets, and a noise matrix, respectively.

Matrix \mathbf{D} can be decomposed into a sparse matrix and a low-rank matrix using Go Decomposition (GoDec) algorithm, as presented by [18], [23].

$$\begin{cases} \min_{\mathbf{L}, \mathbf{S}} \|\mathbf{D} - \mathbf{L} - \mathbf{S}\|_F^2 \\ s.t. \text{rank}(\mathbf{L}) \leq r, \\ \text{card}(\mathbf{S}) \leq \varepsilon \end{cases} \quad (9)$$

where $\|\cdot\|_F$, $\text{rank}(\cdot)$, $\text{card}(\cdot)$ denotes the Frobenius norm, the rank operator, and the cardinality of the sparse matrix, respectively. The variable r represents rank of \mathbf{L} , while the variable ε represents the sparse degree of \mathbf{S} .

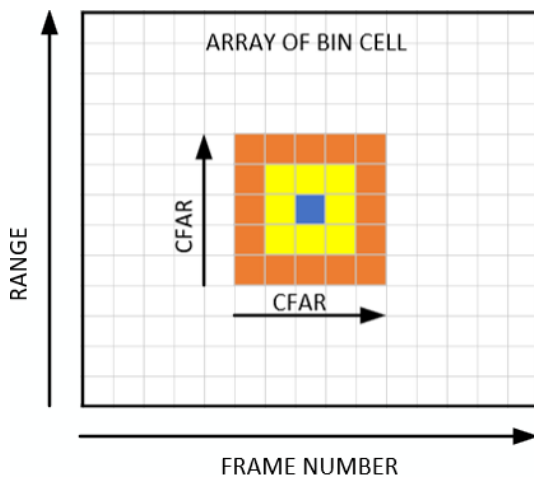


Figure 3. 2D-CFAR structure

III. SYSTEM DESIGN

A. Radar Parameters

The radar target is modeled with a square aluminum plate with dimensions of 2.4×1.2 meters and a height of 2.2 meters above the railway track from a center plate, as shown in Figure 4. Radar Cross Section (RCS) is the ability of a target to reflect the radar signal towards the source of the radar transmitter. The RCS value for a flat target surface following equation (10) is $\pm 1000 \text{ m}^2$. The development of FMCW radar parameters is tabulated in Table 1.

$$\sigma_{\max} = \frac{4\pi w^2 h^2}{\lambda^2} \quad (10)$$

The maximum detection range of developed FMCW radar can be expressed as (11). From (11), assuming $f_{b\max} = F_s$, the maximum detection range (R_{\max}) is 5.6 km which is proper with a minimum detection range as described in [13], while the range resolution of the target is 2.7 m, calculated by equation (12).

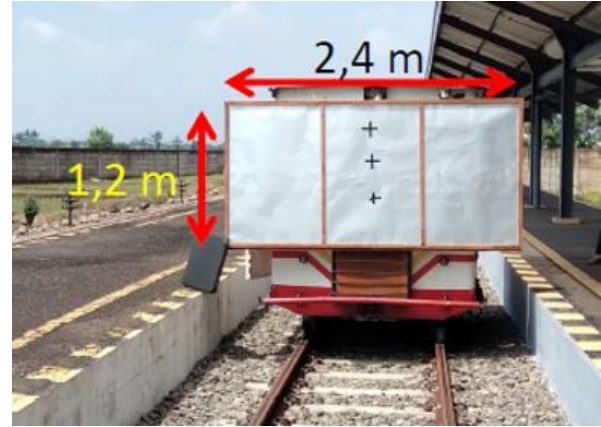


Figure 4. Model target

TABLE 1
FMCW RADAR SIGNAL PARAMETERS

Parameter	Value
Bandwidth (Bw)	54 MHz
Max beat frequency ($f_{b\max}$) = Sampling Frequency (F_s)	2.0833 MHz
Carrier Frequency (F_c)	9.3 GHz
Number of samples (N_{sample})	2048
Number of sweeps (N_{sweep})	8
Time sweep (T_{sweep})	983.04 μs
ADC resolution	12 bits
Horizontal beamwidth	4.3°
Gain Antenna Tx, Rx	21.5 dB
Sidelobe level	11.9 dB
Antenna height above the railway track	1.6 m

$$R_{max} = \frac{C \times T_{sweep} \times f_{bmax}}{2 \times B_w} \quad (11)$$

$$\Delta R = \frac{c}{2 \times B_w} \quad (12)$$

B. Radar Signal Processing

This research divides radar signal processing into four main parts; pre-processing, range processing, detection, and post-processing, as presented in Figure 5. Raw data is collected from ADC 12-bits with a sampling rate of 2.0833 MHz. The total number of sample data in a single sweep is 2048. Collected data will be processed after eight sweeps. Pre-processing steps include dc removal and I/Q imbalance correction. DC component from the received signal is removed by the DC removal step, while I/Q imbalance correction is implemented to reduce mirror signal from unbalancing signal from the output I/Q mixer. After I/Q imbalance correction, range processing is done by Fast Fourier Transform (FFT) with 2048 points.

Implementing Hamming windows before the FFT function to reduce the side lobe signal. Data from FFT named A-scan are collected following recorded time to matrix $Q \times R$ named B-Scan or range profile image. After B-Scan is composed, 2D-CFAR is applied to detect obstacles under noise and low clutter. In this research, 2D-CA and 2D-GOCA CFAR performance is evaluated. Finally, robust principal component analysis is applied to reduce strong clutter that still exists after 2D-CFAR processing.

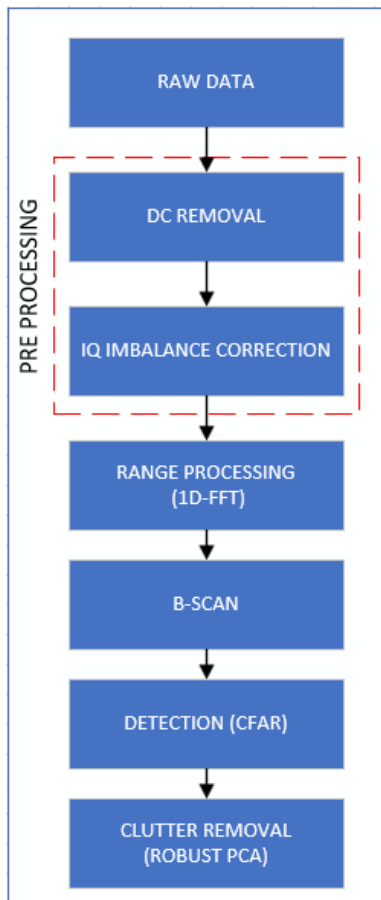


Figure 5. Radar signal processing

IV. RESULTS AND DISCUSSION

A. FMCW Radar Modeling

The detection performance of CFAR has been simulated based on radar parameters as tabulated in Table 1. The simulation scenarios consist of a homogenous and non-homogenous environment to meet the actual condition of the railway track. Four objects are put in different locations (280 m, 400 m, 730 m, and 1000 m) not close to each other. CA and GOCA-CFAR processor are evaluated for both scenarios with SNR=15 dB and CFAR parameters set as follows: $N = 16$, $GC = 2$, $P_{fa} = 1e - 1$, as shown in Figure 9. In Figure 9(a), CA and GOCA CFAR perform well under a homogenous environment. In the second scenario, a clutter edge was added to the signal between the first and second objects. Clutter edge represents clutter signal from surrounding areas of railway track such as building and entrance station building. Figure 9(b) shows that GOCA outperforms CA-CFAR in a non-homogenous environment. CA-CFAR detect more clutter wall than GOCA-CFAR. Both CA and GOCA-CFAR performance depend on the selected reference window N and P_{fa} . In actual application, the trade-off between reference window N and P_{fa} is needed to achieve optimum performance.

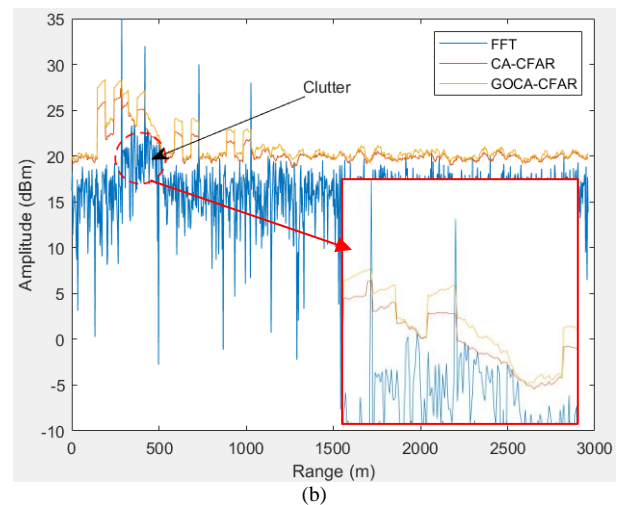
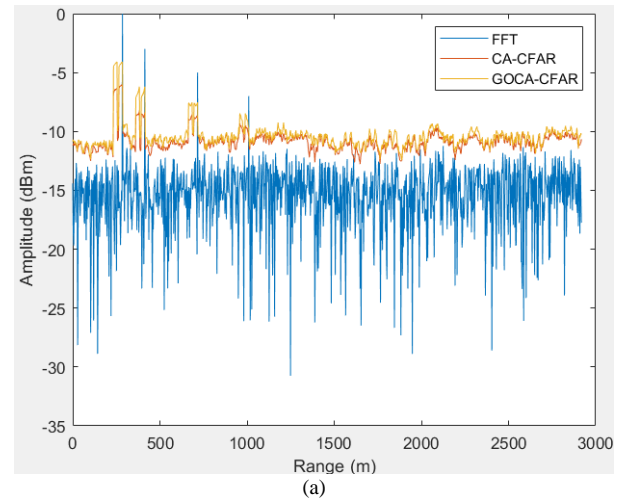


Figure 6. Performance simulation of CA and GOCA-CFAR under (a) homogenous and (b) non-homogeneous environment

B. FMCW Radar Detection

In this work, the measurement setup has been conducted at Cipeuyeuem Stasiun, Cianjur Regency, as shown in Figure 7. The radar antenna's height is 1.6m above the railway track. A target can move forward and backward along the railway track with a speed not exceeding 20 km/hour within a 3000 meters range. The measurement scenario is to detect a moving target along a railway track within a specific distance and direction.

From the measurement setup, raw data are collected and analyzed with a radar signal processing algorithm, as shown in Figure 5. Figure 8 shows the range and 1D-CFAR processing result of the collected data radar receiver. Strong-clutters exist in low-range detection areas due to environment building in the station. Both CA and GOCA-CFAR unwell performs to reduce strong clutter. Figure 8 shows that many clutter signals are detected for close and long-range areas along the railway track. Furthermore, target signals in close-range area detection are mixed with strong clutter, so it is not easy to detect using CFAR algorithm. RPCA algorithms proposed to overcome unwell performs CFAR in a strong clutter environment.

Range profile image or B-Scan is used to analyze moving target detection. B-Scan is composed of several A-scan to a single image. In this research, 360 frames are collected to generate B-Scan. Figure 9 shows a range profile image from the moving target scenario. A moving target path is indicated with a slope line, while a clutter signal is represented with a straight line. Two-dimensional CA and GOCA CFAR performance are analyzed to detect targets in B-scan; the result is shown in Figure 10. 2D-CA and GOCA CFAR parameters are set as follows: $N = 16$, $GC = 2$, $P_{fa} = 1e - 0.8$. Figure 10 shows that 2D-CA and 2D-GOCA CFAR processing can detect a moving target at 250 cells equal to $250 \times 2.7m = 675m$, where 2.7m is radar range resolution. However, strong clutters are still detected at under 50, 90, 130, and 160 cells.

A robust principal component analysis (RPCA) algorithm is implemented to overcome the strong clutters problem. RPCA extract B-scan matrix data to a low-rank



Figure 7. Measurement set-up at Cipeuyeuem station

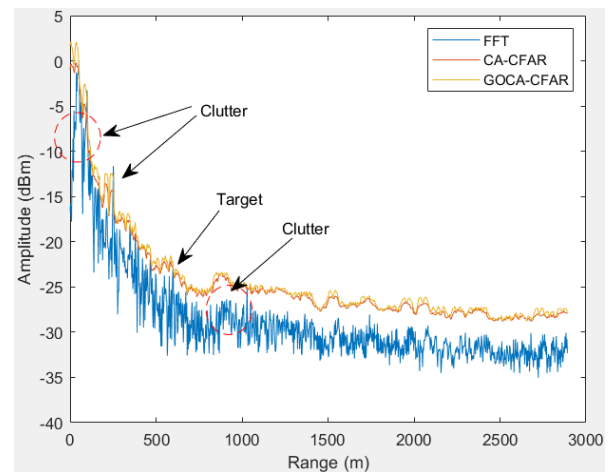


Figure 8. 1D-CFAR processing

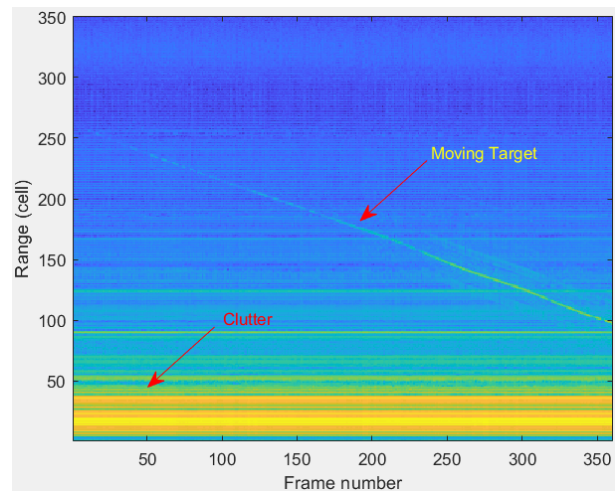


Figure 9. B-Scan or range profile image

clutter matrix L , and a sparse matrix S representing the moving target. By following equation (9), the result of 2D-CFAR, as shown in Figure 10, is extracted into two component matrices. The final result of RPCA process is shown in Figure 11. Figure 11 (a) and (b) show sparse matrix S after two-dimensional CA and CAGO CFAR processing, respectively. The sparse matrix S shows a moving target, while extracted clutter is shown in Figure 11(c) as a low-rank matrix L . The moving target in sparse matrix S is sometimes not detected due to the received signal being too weak, and the railway track altitude is not the same point. In another way, the clutter removal performance of the average background subtraction algorithm is shown in Figure 12. Figure 12 shows that much clutter is still detected due to the amplitude power of clutter greater than the average background clutter power. At this point, RPCA can effectively extract a moving target from clutter with a limited condition, such as the target in slow motion in case the experiment use speed does not exceed 20 km/hour. For future research, more data should be collected with varying speeds up to 300 km/hour to verify that algorithm can be implemented in a high-speed moving target.

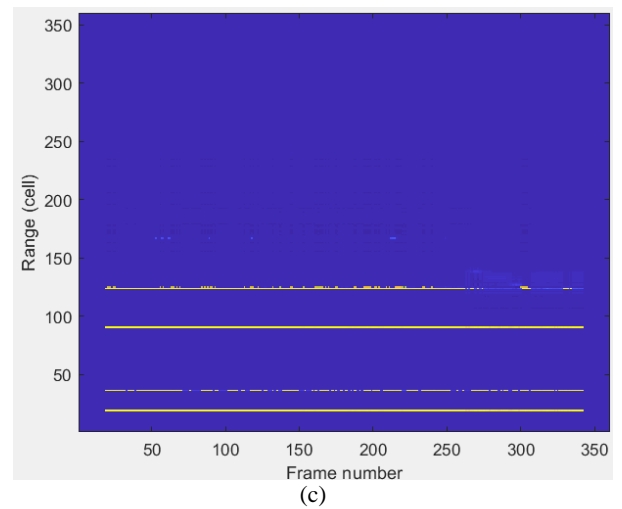
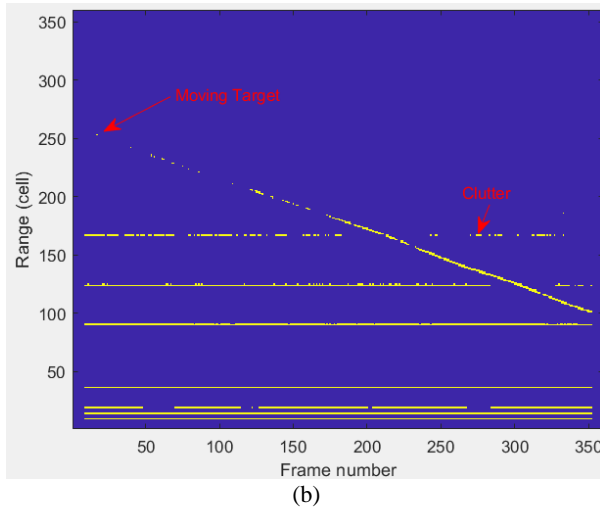
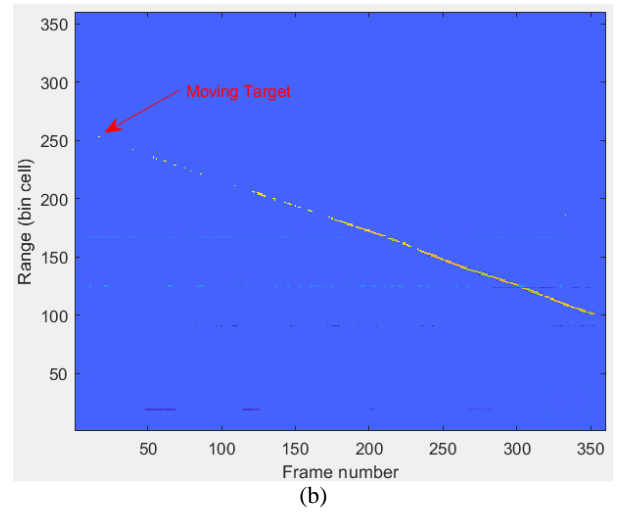
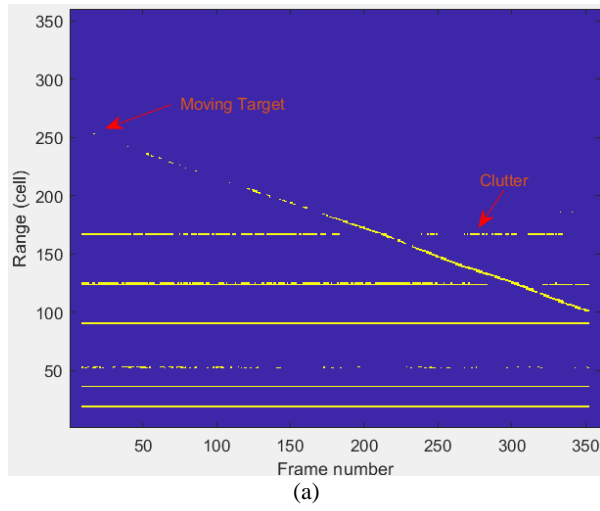


Figure 10. 2D-CFAR performance (a) 2D-CA-CFAR, (b) 2D-GOCA-CFAR

Figure 11. RPCA performance, (a) sparse matrix S after 2D-CA-CFAR, (b) sparse matrix S after 2D-GOCA-CFAR, (c) low-rank matrix L after 2D-CA-CFAR

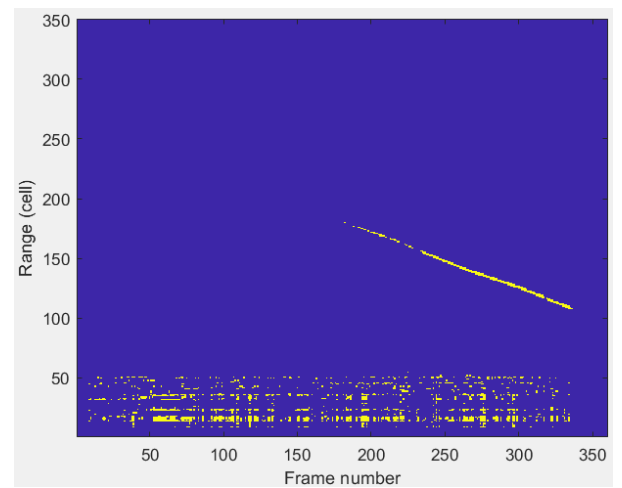
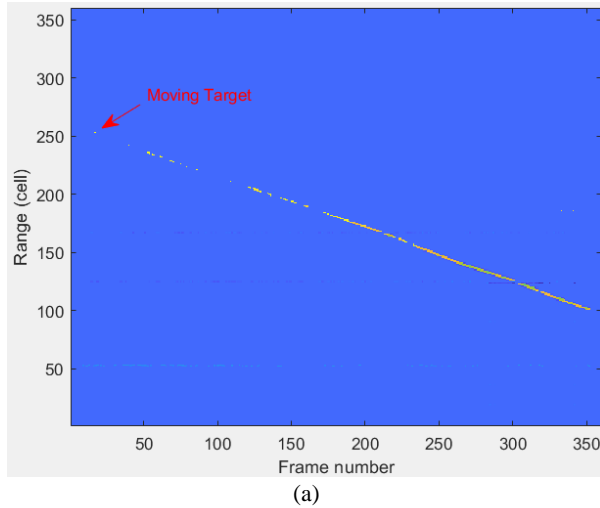


Figure 12. Clutter removal performance from combining 2D-CFAR and average background subtraction

V. CONCLUSION

FMCW radar signal processing for railway collision avoidance has been evaluated in various scenarios. From the analyzed data on simulation and actual measurement, performance detection depends on the signal-to-noise ratio and trade-off CFAR threshold under various

conditions. Combining 2D-CFAR and RPCA algorithms can extract moving targets under clutter effectively. From the measurement, the development of FMCW radar can detect an obstacle or target of 675 meters. The detection target range should be improved to 3000 meters for future research to meet the requirement of a safety braking system in a high-speed railway to prevent a collision.

DECLARATIONS

Conflict of Interest

The authors have declared that no competing interests exist.

CRedit Authorship Contribution

Farra Anindya Putri: Software, writing original draft preparation; Dayat Kurniawan: Software, Writing - Review & Editing, Conceptualization, Methodology, Investigation; Rahmawati Hasanah: supervision; Taufiqurrahman, Eko Joni Priyanto, Hana Arisesa, Deni Permana, Winy Desvasari, Ken Paramayudha, Arief Budi Santiko, Dadin Mahmudin, Pamungkas Daud, Fajri Darwis, Erry Dwi Kurniawan: Conceptualization, Methodology, Investigation; Yusuf Nur Wijayanto: Supervision, Conceptualization, Methodology, Investigation; Tajul Miftahushudur, Prasetyo Putranto, Arie Setiawan: Software; Syamsu Ismail: supervision, Conceptualization, Methodology, Investigation.

Funding

This research is fully funded and supported by National Priority Program (PRN) Indonesia Endowment Fund for Education (LPDP).

Acknowledgment

This research is fully supported by Research Center for Telecommunication National Research and Innovation Agency, Research Center for Electronics National Research and Innovation Agency, Stationmaster, and crew of Cipeyeum Station, Faculty of Electrical Engineering Telkom University.

REFERENCES

- [1] T. Dhanabalu, S. Sugumar, S. Suryaprakash, and A. Vijayanand, "Sensor based identification system for train collision avoidance," *ICIIECS 2015 - 2015 IEEE Int. Conf. Innov. Information, Embed. Commun. Syst.*, pp. 0–3, 2015, doi: 10.1109/ICIIECS.2015.7192995.
- [2] Y. Gao, H. Xu, J. Gao, and J. Du, "Research of sds-twr ranging based on collision avoidance of anti-collision warning system in urban rail train," in *2017 12th IEEE Conf. Ind. Electron. Appl.*, 2017, pp. 218–220. doi: 10.1109/ICIEA.2017.8282845.
- [3] S. S. Bhavsar and A. N. Kulkarni, "Train collision avoidance system by using rfid," in *2016 Int. Conf. Comput. Anal. Secur. Trends*, 2016, pp. 30–34. doi: 10.1109/CAST.2016.7914935.
- [4] B. Mishra, "TMCAS: an mqtt based collision avoidance system for railway networks," in *2018 18th Int. Conf. Comput. Sci. Appl.*, 2018, pp. 1–6. doi: 10.1109/ICCSA.2018.8439562.
- [5] F. Shouyong, Z. Jimin, X. Lichao, Z. Zhenhai, and L. Jinnan, "Rail identification using camera and millimeter-wave radar data," in *2021 Int. Conf. Inf. Technol. Biomed. Eng.*, 2021, pp. 150–154. doi: 10.1109/ICITBE54178.2021.00041.
- [6] A. K. Kyatsandra, R. K. Saket, S. Kumar, K. Sarita, A. S. S. Vardhan, and A. S. S. Vardhan, "Development of trineta: a sensor based vision enhancement system for obstacle detection on railway tracks," *IEEE Sens. J.*, vol. 22, no. 4, pp. 3147–3156, 2022, doi: 10.1109/JSEN.2021.3140032.
- [7] M. Karaduman, "Image processing based obstacle detection with laser measurement in railways," in *2017 10th Int. Conf. Electr. Electron. Eng.*, 2017, pp. 899–903.
- [8] H. Mukojima *et al.*, "Moving camera background-subtraction for obstacle detection on railway tracks," in *2016 IEEE Int. Conf. Image Process.*, 2016, pp. 3967–3971. doi: 10.1109/ICIP.2016.7533104.
- [9] C. Wisultschew, G. Mujica, J. M. Lanza-Gutierrez, and J. Portilla, "3D-lidar based object detection and tracking on the edge of iot for railway level crossing," *IEEE Access*, vol. 9, pp. 35718–35729, 2021, doi: 10.1109/ACCESS.2021.3062220.
- [10] K. Lee, E. Chae, S. Oh, and J. Hwang, "Study on train collision avoidance system for securing safe distance between trains," in *2013 Int. Conf. Electr. Mach. Syst.*, 2013, pp. 1342–1344. doi: 10.1109/ICEMS.2013.6713274.
- [11] J. Yanwei and D. Yu, "Research on railway obstacle detection method based on radar," *Proc. - 2021 7th Int. Symp. Mechatronics Ind. Informatics, ISMII 2021*, pp. 222–226, 2021, doi: 10.1109/ISMII52409.2021.00054.
- [12] A. Liu, Q. Yang, X. Zhang, and W. Deng, "Collision avoidance radar system for the bullet train: implementation and first results," *IEEE Aerosp. Electron. Syst. Mag.*, vol. 32, no. 5, pp. 4–17, 2017, doi: 10.1109/MAES.2017.150104.
- [13] L. He, "Study on brake mode for 300km/h electric motor train unit with distributed power," *Railw. Locomot. & Car*, 2003.
- [14] H. M. Finn, "Adaptive detection mode with threshold control as a function of spatially sampled clutter level estimates," 1968.
- [15] M. K. Uner and P. K. Varshney, "CFAR processing in nonhomogeneous background," in *Proc. MELECON '94. Mediterr. Electrotech. Conf.*, 1994, pp. 156–159 vol.1. doi: 10.1109/MELCON.1994.381120.
- [16] V. G. Hansen and J. H. Sawyers, "Detectability loss due to 'greatest of' selection in a cell-averaging cfar," *IEEE Trans. Aerosp. Electron. Syst.*, vol. AES-16, no. 1, pp. 115–118, 1980, doi: 10.1109/TAES.1980.308885.
- [17] M. A. Richards, *Fundamentals Of Radar Signal Processing*. McGraw-Hill Education (India) Pvt Limited, 2005. [Online]. Available: <https://books.google.co.id/books?id=qizdSv8MEngC>
- [18] J. Su *et al.*, "A novel multi-scan joint method for slow-moving target detection in the strong clutter via rpca," in *2021 IEEE Int. Geosci. Remote Sens. Symp. IGARSS*, 2021, pp. 4787–4789. doi: 10.1109/IGARSS47720.2021.9554191.
- [19] D. Yang, G. Liao, S. Zhu, and X. Yang, "RPCA based moving target detection in strong clutter background," in *2015 IEEE Radar Conf.*, 2015, pp. 1487–1490. doi: 10.1109/RADAR.2015.7131231.
- [20] J. Abdullah and M. S. Kamal, "Multi-targets detection in a non-homogeneous radar environment using modified ca-cfar," in *2019 IEEE Asia-Pacific Conf. Appl. Electromagn.*, 2019, pp. 1–5. doi: 10.1109/APACE47377.2019.9020820.
- [21] M. Kronauge and H. Rohling, "Fast two-dimensional cfar procedure," *IEEE Trans. Aerosp. Electron. Syst.*, vol. 49, no. 3, pp. 1817–1823, 2013, doi: 10.1109/TAES.2013.6558022.
- [22] X. Song, D. Xiang, K. Zhou, and Y. Su, "Improving rpca-based clutter suppression in gpr detection of antipersonnel mines," *IEEE Geosci. Remote Sens. Lett.*, vol. 14, no. 8, pp. 1338–1342, 2017, doi: 10.1109/LGRS.2017.2711251.
- [23] T. Zhou and D. Tao, "GoDec: randomized lowrank & sparse matrix decomposition in noisy case," in *Proc. 28th Int. Conf. Mach. Learn. ICML 2011*, 2011, pp. 33–40.